JOURNAL OF THE
CHUNGCHEONG MATHEMATICAL SOCIETY
Volume **31**, No. 1, February 2018
http://dx.doi.org/10.14403/jcms.2018.31.1.137

THE FAST TRUNCATED LAGRANGE METHOD FOR IMAGE DEBLURRING WITH ANTIREFLECTIVE BOUNDARY CONDITIONS

SeYoung Oh* and SunJoo Kwon**

Abstract. In this paper, under the assumption of the symmetry point spread function, antireflective boundary conditions(AR-BCs) are considered in connection with the fast truncated Lagrange(FTL) method. The FTL method is proposed as an image restoration method for large-scale ill-conditioned BTTB(block Toeplitz with Toeplitz block) and BTHHTB(block Toeplitz-plus-Hankel matrix with Toeplitz-plus-Hankel blocks) linear systems([13, 17]). The implementation and efficiency of the FTL method in the AR-BCs are further illustrated. Especially, by employing the AR-BCs, both the continuity of the image and the continuity of its normal derivative are preserved at the boundary. A reconstructed image with less artifacts at the boundary is obtained as a result.

1. Introduction

The discrete mathematical model of blurred image gives an equation

$$Af = y, \tag{1.1}$$

where y is the observed image. A large scale ill-conditioned matrix A blurring the unknown true image f is modeled with the spatially invariant discrete point spread function(PSF).

To find an useful approximation of the true image, the discrete ill-posed problems of the image reconstruction frequently use a Tikhonov regularization form

$$\min_f \|Af - y\|_2^2 + \lambda \|f\|_2^2 , \tag{1.2}$$

Received November 28, 2017; Accepted January 28, 2018.
2010 Mathematics Subject Classification: Primary 65F22, 65K10, 65F10.
Key words and phrases: fast truncated Lagrange method, image reconstruction, reflective BCs, antireflective BCs, constrained linear least-square problems, discrete cosine transform, discrete sine transform.

Correspondence should be addressed to SunJoo Kwon, sjkw@cnu.ac.kr.

where λ is a positive regularization parameter.

The purpose of deblurring problem is to recover the true image from blurred and noisy images. Because of the blurring process, the boundary values of degraded image are not completely determined by the original image inside the scene. The choice of the most reasonable boundary condition is an important aspect in the modelization of image blurring.

The PSF matrix imposed antireflective boundary conditions(AR-BCs) is related to a Toeplitz+Hankel plus 2 rank correction matrix, where the corrections are placed at the first and the last column. This matrix is not diagonalizable by unitary transformations including the case of quadrantally symmetric blur. Nevertheless, it is possible to transform it into a simple matrix by means of trigonometric transforms by using two different approaches in [3]. These approaches are based on the fact that the eigenvector basis of the antireflective matrix of order n is made by $n-2$ sine frequency functions and 2 more linear functions. In particular, the latter linear functions are low frequencies associated with the eigenvalue one of multiplicity two. To exploite this property, in [3] the components corresponding to the linear eigenvectors are first reconstructed. Then the remaining problem of order $n-2$ is diagonalized by the discrete sine transform. At the boundary the continuity of the image and its normal derivative (C^1 continuity)are preserved by the AR-BCs. Therefore typical artifacts called ringing effects are negligible with respect to the other BCs[19], at least for piecewise smooth images.

The fast truncated Lagrange(FTL) method is well suited for large-scale ill-conditioned BTTB(block Toeplitz with Toeplitz block) and BTHHTB(block Toeplitz-plus-Hankel matrix with Toeplitz-plus-Hankel blocks) linear systems which is from an image restoration problem with zero and reflective boundary condition ([13, 17]). FTL method uses a quasi-Newton method applying to the first-order optimality conditions of the Lagrangian function for the equality constrained minimization of (1.2). Since the Hessian of the Lagrangian can be approximated by a BCCB (block circulant with circulant block) and BTHHTB matrix, the two-dimensional fast Fourier transform(FFT) and Discrete cosine transform (DCT) are used to compute the quasi-Newton step. The quasi-Newton iteration is terminated according to the discrepancy principle. The corresponding Lagrange multiplier of an iterative Lagrange method acts as a regularization parameter.

For the purpose of comparing for the AR-BCs with the reflective BCs, we tested three images in [9] and two blurring models, *Gaussian* model and *out-of-focus* blurring model, are used as in [10, 11]. According to the computed results with our algorithm written by Matlab, all three test images in our experiment gave the smaller relative accuracies and the higher PSNR under the AR-BCs, and thus, the more quality image under the AR-BCs than reflective BCs. And there are little ringing effect in the reconstructed images from the AR-BCs.

In this paper, the FTL-method is applied to the image restoration problem with the AR-BCs. The outline of this paper is organized as follows: Section 2 recalls the characteristics of AR-BCs. Section 3 describes the usage of the AR-BCs in the FTL method. The related simulation is illustrated in Section 4. Finally, Section 5 concludes this paper.

2. The Antireflective Matrices

In this section, the structure of the matrix A representing the blurring operator with the AR-BCs in [1, 2, 5, 6, 7] are reviewed.

Let $Q_n^{(1)}$ be the n-dimensional discrete sine transform(DST I), orthogonal and symmetric matrix:

$$(Q_n^{(1)})_{ij} = \sqrt{\frac{2}{n+1}} \sin(\frac{ji\pi}{n+1}), i, j = 1, \ldots, n. \tag{2.1}$$

And let $Q_n^{(d)} = Q_n^{(1)} \otimes \cdots \otimes Q_n^{(1)}$ be d (≥ 1) time Kronecker products of $Q_n^{(1)}$. Then we define $\tau_n^{(d)}$ to be the space of all the matrices that can be diagonalized by $Q_n^{(d)}$:

$$\tau_n^{(d)} = \{Q_n^{(d)} D Q_n^{(d)} : D \text{ is a real diagonal matrix of size } n^d\}.$$

The classes of $n^d \times n^d$ matrices $\mathcal{S}^{(d)}$ is defined by the following. For $d = 1$, $A \in \mathcal{S}^{(1)}$ if

$$A = \begin{pmatrix} \alpha & & \\ v & \widehat{A} & w \\ & & \beta \end{pmatrix},$$

with $\alpha, \beta \in \mathbf{R}$, $\mathbf{v}, \mathbf{w} \in \mathbf{R}^{n-2}$ and $\widehat{A} \in \tau_{n-2}^{(1)}$. For $d > 1$, $A \in \mathcal{S}^{(d)}$ if

$$A = \begin{pmatrix} \alpha & & \\ \mathbf{v} & A^* & \mathbf{w} \\ & & \beta \end{pmatrix},$$

with $\alpha, \beta \in \mathcal{S}^{(d-1)}, \mathbf{v}, \mathbf{w} \in \mathbf{R}^{(n-2)n^{d-1} \times n^{d-1}}$, $\mathbf{v} = (v_j)_{j=1}^{n-2}$, $\mathbf{w} = (w_j)_{j=1}^{n-2}$, $v_j, w_j \in \mathcal{S}^{(d-1)}$, and $A^* = (A^*_{i,j})_{i,j=1}^{n-2}$ having an external $\tau_{n-2}^{(1)}$ structure, with $A^* = (A^*_{i,j}) \in \mathcal{S}^{(d-1)}$.

For the case of one dimensional($d = 1$) objects, the spectral decomposition of the coefficient matrix obtained by imposing AR-BCs is described by using the AR(antireflective)-transform in [1, 7].

AR-BCs are imposed by a central symmetry around the boundary point by $f_{1-j} = f_1 - (f_{j+1} - f_1) = 2f_1 - f_{j+1}$, and $f_{n+j} = f_n - (f_{n-j} - f_n) = 2f_n - f_{n-j}$, for $j = 1, \dots, m$. Then (1.1) becomes

$$Af = \left[ze_1^T - (0|T_l)\widetilde{J} + T - (T_r|0)\widehat{J} + we_n^T\right] f = y, \tag{2.2}$$

where e_k is the kth vector of the canonical basis $\widetilde{J} = \begin{pmatrix} 0 & 0 \\ 0 & J \end{pmatrix}$, $\widehat{J} = \begin{pmatrix} J & 0 \\ 0 & 0 \end{pmatrix}$ with J denoting the $(n-1)$-dimensional flip matrix and the matrices T_l, T, and T_r are lower triangular Toeplitz, Toeplitz, and upper triangular Toeplitz respectively. The linear system (2.2) can be solved by using three FST in $O(n \log n)$ operations ([19]).

If a PSF $\mathbf{h} = \begin{pmatrix} h_{-m} & \dots & h_0 & \dots & h_m \end{pmatrix}$ is symmetric and $\sum_{j=-m}^{m} h_j = 1$, the precise structure of the coefficient A in (2.2) is Toeplitz+Hakel plus 2 rank correction matrix

$$A = \begin{pmatrix} z_1 + h_0 & 0 \ \dots \ 0 & 0 \\ z_2 + h_1 & & 0 \\ \vdots & & h_m \\ z_m + h_{m-1} & \widehat{A} & z_m + h_{m-1} \\ h_m & & \vdots \\ 0 & & z_2 + h_1 \\ 0 & 0 \ \dots \ 0 & z_1 + h_0 \end{pmatrix}, \tag{2.3}$$

where $A_{1,1} = A_{n,n} = 1, z_j = 2\sum_{k=j}^{m} h_k, \widehat{A} \in \tau_{n-2}^{(1)}$.

The eigenvalues of the $\tau_{n-2}^{(1)}$ matrix as indicated in [1] are given by the cosine function $h(x)$ evaluated at the grid point $x_i = i\pi/(n-1)$ for $i = 1, \dots, n-2$,

$$h(x) = \sum_{j=-m}^{m} h_j e^{ijx}, i = \sqrt{-1}. \tag{2.4}$$

LEMMA 2.1. [19] *For the symmetric blurring function h, the matrix $\widehat{A}$ in (2.3) can be diagonalized by $Q_{n-2}^{(1)}$;*

$$\widehat{A} = (Q_{n-2}^{(1)})^H diag(h(\mathbf{x})) Q_{n-2}^{(1)},$$

and $\widehat{A} = PAP^T$ *with*

$$P = \begin{pmatrix} 0 & & 0 \\ \vdots & I_{n-2} & \vdots \\ 0 & & 0 \end{pmatrix} \in R^{(n-2)\times n}.$$

Also, the eigenvalues of A *are given by* 1 *with multiplicity* 2 *and by the eigenvalues of* $\widehat{A}$.

Note that the eigenvalues $h(x_i)$ can be easily computed by $D_{i,i} = \frac{[Q^{(1)}_{n-2}(\widehat{A}e_1)]_i}{[Q^{(1)}_{n-2}e_1]_i}$, $i = 1, \ldots, n-2$. That is, applying a DST I transform to the first column of $\widehat{A}$, the eigenvalues of $\widehat{A}$ can be founded.

In [1, 7], the AR-transform is defined by the matrix

$$T_n = \begin{pmatrix} \alpha_n^{-1} & & 0 \\ \alpha_n^{-1}\mathbf{p} & Q^{(1)}_{n-2} & \alpha_n^{-1}J\mathbf{p} \\ 0 & & \alpha_n^{-1} \end{pmatrix}, \tag{2.5}$$

where the vector $\widetilde{\mathbf{p}} = [1, \mathbf{p}^T, 0]^T$ is the sampling of the function $1 - x$ on the grid $j/(n-1)$ for $j = 0, \ldots, n-1$, $\alpha_n = \|\widetilde{\mathbf{p}}\|_2 = \sqrt{\frac{n(2n-1)}{6(n-1)}}$ and J is the $n-2$ dimensional flip matrix, i.e., $[J]_{s,t} = 1$ if $s + t = n - 1$ and zero otherwise. The inverse of the AR-transform is obtained as

$$T_n^{-1} = \begin{pmatrix} \alpha_n & & 0 \\ -Q^{(1)}_{n-2}\mathbf{p} & Q^{(1)}_{n-2} & -Q^{(1)}_{n-2}\mathbf{p} \\ 0 & & \alpha_n \end{pmatrix}. \tag{2.6}$$

The spectral decomposition of the antireflective matrix A in (2.3) is

$$A = \mathcal{A}_n(h) = T_n D_n T_n^{-1}, \tag{2.7}$$

where $D_n = diag(h(x))$ with x defined as $x_1 = x_n = 0$ and $x_{j+1} = \frac{j\pi}{n-1}$ for $j = 1, \ldots, n-2$.

Tikhonov regularization problem (1.2) can be rewritten as the linear system

$$(A^T A + \lambda I)f = A^T y, \tag{2.8}$$

which has an unique solution. For the matrix A under AR-BCs, since $A^T \neq A$ even for a symmetric PSF and the antireflective algebra is not closed under transposition, it was proposed to replace A^T by A in regularization process in [4]. Thus the associated Tikhonov linear system becomes $(A^2 + \lambda I)f = Ay$ and the reblurring equation to be solved becomes

$$\mathcal{A}_n(h^2 + \lambda)f = \mathcal{A}_n(h)y. \tag{2.9}$$

Generally, the expanding matrix with AR-BCs in d-level case is described as follows.

THEOREM 2.2. [2] *Let h be the d-dimensional PSF then the $n^d \times n^d$ blurring matrix A with $n \geq 3$ and AR-BCs has the form*

$$A = \begin{pmatrix} z_1 + h_0 & 0 \ \dots \ 0 & 0 \\ z_2 + h_1 & & 0 \\ \vdots & & h_m \\ z_m + h_{m-1} & A^* & z_m + h_{m-1} \\ h_m & & \vdots \\ 0 & & z_2 + h_1 \\ 0 & 0 \ \dots \ 0 & z_1 + h_0 \end{pmatrix}, \tag{2.10}$$

where zeros denote null matrices of proper order, where

1. $h_j \in R^{n^{d-1} \times n^{d-1}}$ *is the AR-BC matrix related to the $(d-1)$-dimensional PSF* $\mathbf{h}^{(d)}_{(d-1,\{1\},j)} = (h_{j,k})^m_{k_1,\dots,k_{d-1}=-m}$ *and* $z_j = 2\sum_{k=j}^m h_k$.
2. $A \in \mathcal{S}^{(d)}$.

In [6], it was shown that matrix operations such as inversion, matrix vector product, computation of the eigenvalues, and solving linear systems can all be done by using a constant number of d-level sine transforms, and therefore the resulting cost is $O(n^d \log n)$.

If h is a d-variate real-valued cosine symbol related to the d-dimensional symetric and normalized mask $\mathbf{h}$, then

$$A = \mathcal{A}_n(h) = T_n^{(d)} D_n (T_n^{(d)})^{-1}, T_n^{(d)} = T_n \otimes \cdots \otimes T_n$$

where D_n is a diagonal matrix containing the eigenvalues of $\mathcal{A}_n(h)$.

3. The Fast Truncated Lagrange Method for AR-BCs

This section investigates the fast truncated Lagrange(FTL) method method for the image restoration problem with the antireflective boundary condition. The FTL method does not require any prior good estimates of the regularization parameter. The detailed information regarding FTL method is further discussed in [13].

To minimize the problem (1.2), the equality constrained minimization,

$$\begin{aligned} &\min_{f} && \frac{1}{2}\left\|f\right\|^2 \\ &\text{subject to} && \frac{1}{2}\left\|Af-y\right\|^2 = \epsilon, \end{aligned} \tag{3.1}$$

can be solved for f. The ϵ is a small positive parameter such as $0 < \epsilon \ll \frac{\delta^2}{2}$ if δ is explicitly known as the error. The problem (3.1) is replaced with the unconstrained minimization problem of the Lagrangian function $L(f, \lambda)$, where the Lagrangian function for (3.1) is

$$L(f,\lambda) = \frac{1}{2}\left\|f\right\|^2 + \lambda\left(\frac{1}{2}\left\|Af-y\right\|^2 - \epsilon\right) \tag{3.2}$$

and λ the Lagrange multiplier. The Hessian matrix of $L(f, \lambda)$ is $\nabla^2_{ff}L(f, \lambda) = I + \lambda A^T A$. By applying the first order optimality conditions for this problem, the new constrained minimization problem

$$\begin{aligned} &\min_{f,\lambda} && L(f,\lambda) \\ &\text{subject to} && \nabla_{f,\lambda}L(f,\lambda) = 0, \lambda \geq 0 \end{aligned} \tag{3.3}$$

is obtained. Let $k(f) = \frac{1}{2}\left\|Af - y\right\|^2 - \epsilon$. The iterative solution of the above problem can be drived as in the following theorem.

THEOREM 3.1. *The iterative solution of problem (3.3) with antireflective BCs in the FTL method is*

$$f_{i+1} = f_i + \Delta f, \lambda_{i+1} = \lambda_i + \Delta\lambda, \tag{3.4}$$

where the search direction $(\Delta f^T, \Delta\lambda)$ *is*

$$\begin{aligned} \Delta\lambda &= (\nabla_f k(f_i)^T \mathcal{A}_n(1+\lambda h^2)^{-1}\nabla_f k(f_i))^{-1}\{k(f_i) \\ &\qquad - \nabla_f k(f_i)^T \mathcal{A}_n(1+\lambda h^2)^{-1}\nabla_f L(f_i,\lambda_i)\}, \\ \Delta f &= -\mathcal{A}_n(1+\lambda h^2)^{-1}(\nabla_f L(f_i,\lambda_i) + \nabla_f k(f_i)\Delta\lambda). \end{aligned} \tag{3.5}$$

Proof. The coefficient matrix A obtained by considering antireflective BCs is related to a Toeplitz+Hankel plus a structured low rank matrix. Thus it needs to replace A^T by A. The Hessian of $L(f, \lambda)$ can be approximated by $\mathcal{A}_n(1+\lambda h^2)$ which is symmetric and positive definite. From a truncated Taylor series expansions of $\nabla_{f,\lambda}L(f_{i+1}, \lambda_{i+1})$ about (f_i^T, λ_i),

$$\begin{aligned} &\nabla_{f,\lambda}L(f_i+\Delta f, \lambda_i + \Delta\lambda) \\ &\approx \nabla_{f,\lambda}L(f_i,\lambda_i) + \begin{pmatrix} \mathcal{A}_n(1+\lambda h^2) & \nabla_f k(f_i) \\ \nabla_f k(f_i)^T & 0 \end{pmatrix}\begin{pmatrix} \Delta f \\ \Delta\lambda \end{pmatrix}, \end{aligned} \tag{3.6}$$

we can obtain the system

$$\begin{pmatrix} \mathcal{A}_n(1+\lambda h^2) & \nabla_f k(f_i) \\ \nabla_f k(f_i)^T & 0 \end{pmatrix} \begin{pmatrix} \Delta f \\ \Delta\lambda \end{pmatrix} = -\begin{pmatrix} \nabla_f L(f_i,\lambda_i) \\ k(f_i) \end{pmatrix}. \tag{3.7}$$

The solution $(\Delta f^T, \Delta\lambda)$ of (3.7) becomes the quasi-Newton direction in (3.5). □

The step length α_i can be selected by the first number of $\{\frac{1}{2^{j-1}}\}_{j=1,2,...}$ which satisfies the Armijo's condition:

$$m(f+\alpha\Delta f, \lambda+\alpha\Delta\lambda) \leq m(f,\lambda) + \mu\alpha(\Delta f^T, \Delta\lambda)\nabla_{f,\lambda} m(f,\lambda),$$

where the merit function $m(x,\lambda) = \frac{1}{2}\left\|\nabla_{f,\lambda} L(f,\lambda)\right\|^2$ and $\mu = 10^{-4}$. By including the step length α_i along $(\Delta f^T, \Delta\lambda)$, (3.4) is replaced by

$$f_{i+1} = f_i + \alpha_i \Delta f, \lambda_{i+1} = \lambda_i + \alpha_i \Delta\lambda. \tag{3.8}$$

The iteration (3.8) is stopped if an iterate f_i has been found such that $\|Af_i - y\| \leq \rho\delta$, where $\rho \geq 1$ is a fixed parameter. In case without finding an approximated solution satisfying this condition, the method is terminated when a maximum number Max of iterations has been reached. The basic structure of FTL method for the image deblurring problem with AR-BCs is as follows.

Algorithm 1. FTL algorithm for image deblurring problem with antireflective BCs.

1. Input f_0, λ_0, y, ρ, δ, Max.
2. **For** $i = 0, 1, 2, \ldots$.
   i. Compute
   $$\Delta\lambda = (\nabla_f k(f_i)^T \mathcal{A}_n(1+\lambda h^2)^{-1}\nabla_f k(f_i))^{-1}\{k(f_i) - \nabla_f k(f_i)^T \mathcal{A}_n(1+\lambda h^2)^{-1}\nabla_f L(f_i,\lambda_i)\},$$
   $$\Delta f = -\mathcal{A}_n(1+\lambda h^2)^{-1}(\nabla_f L(f_i,\lambda_i) + \nabla_f k(f_i)\Delta\lambda).$$
   ii. Find the step length α_i along $(\Delta f^T, \Delta\lambda)$.
   iii. $f_{i+1} = f_i + \alpha_i\Delta f$, $\lambda_{i+1} = \lambda_i + \alpha_i\Delta\lambda$.
   iv. If $\|Af_{i+1} - y\| \leq \rho\delta$ or $i \geq Max$, then stop.

4. Experimental Results

This section demonstrates the efficiency of employing AR-BCs over reflective BCs for image restoration problems. Two-dimensional AR-transform(including FSTs) and FCTs are used to compute the restored images for each of the antireflective and the reflective BCs.

Our test images are *planet, text,* and *a* as in [9] and two blurring models are used as in [10, 11]. The first blurring is modeled by the

Gaussian PSF, $A(x-x', y-y') = \frac{1}{2\pi\sigma\bar{\sigma}} \exp\left(-\frac{1}{2}\left(\frac{x-x'}{\sigma}\right)^2 - \frac{1}{2}\left(\frac{y-y'}{\bar{\sigma}}\right)^2\right)$, where $\bar{\sigma}$ and σ are two constants for the blurring in the x and y directions respectively, such as $\sigma = \bar{\sigma} = 5$. The second blurring is the *out-of focus* blur whose PSF is

$$A(x-x', y-y') = \begin{cases} (\pi r^2)^{-1}, & \sqrt{(x-x')^2 + (y-y')^2} \leq r, \\ 0, & otherwise, \end{cases}$$

where the parameter r characterizes the defocus such as $r = 10$. The Matlab code of *psfGauss* and *psfDefocus* are taken from *RestoreTools* package [14].

To measure the quality of the reconstructed image, the relative accuracy, $rel = \frac{\|f_{true} - f_{approx}\|}{\|f_{true}\|}$; and the *PSNR* values of the recovered images, $PSNR = 10 \log 10\left(\frac{255^2}{MSE}\right)$ are used, where $MSE(I, J) = \frac{\Sigma_{i,j}(I(i,j) - J(i,j))^2}{mn}$ is the mean square error for two $m \times n$ monochrome images I and J.

Considering the AR-BCs in the 2-dimensional case, coefficient matrix A in (1.2) becomes a 2-level Toeplitz+Hankel plus a 2-level structured low rank matrix. The bidimensional AR-transform can be defined as

$$T_n^{(2)} = T_n \otimes T_n. \tag{4.1}$$

Thus the coefficient matrix A can be diagonalized,

$$A = \mathcal{A}_n(h) = T_n^{(2)} D_n T_n^{(2)}, \tag{4.2}$$

where h is a bidimensional trigonometric function depending on the coefficient of the PSF, and D_n is a diagonal matrix containing the eigenvalues of $\mathcal{A}_n(h)$.

The Matlab code for the AR-transform, its inverse transform and the computation of the eigenvalues of the antireflective matrix are available at [8]. Especially, the spectrum of A can be computed by using *dARt2*(A) which contains the two-dimensional discrete sine transform *dst2*. Thus the product $y = Af$ is obtained as

$$y = vector\,(idARt2(\,dARt2(A).*\,dARt2(F)))\,,$$

where *idARt2* is the inverse process of *dARt2*. Then the solution $\varpi = (I + \lambda A^T A)^{-1} f \approx \mathcal{A}_n(1 + \lambda h^2)^{-1} f$ is computed as

$$\varpi = vector(idAR2(dARt2(F)./(1 + \lambda dARt2(A).\hat{}2))),$$

where ./ and .^ are the component-wise division and squaring of the matrix *dARt2*(A) respectively.

Figure 1(a) shows the *Gaussian* blurred and noisy image of the *planet*. Figure 1(b) is the reconstructed image under the AR-BCs by FTL

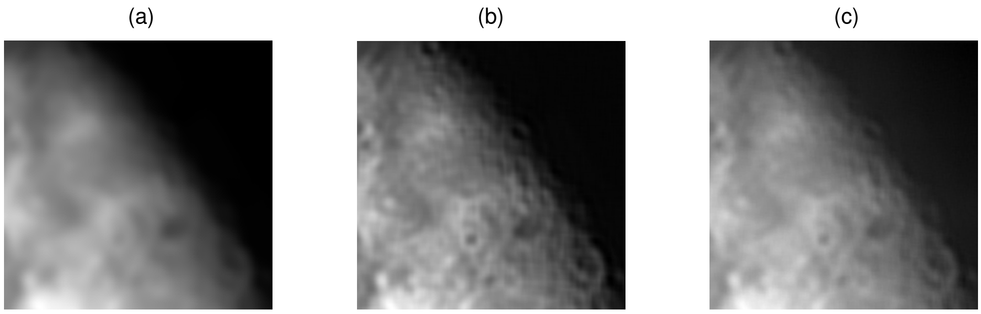

FIGURE 1. *Gaussian* blur : Restored image with (b) AR-BCs ($rel = 7.10\times10^{-2}$, $PSNR = 37.26$) and (c) reflective BCs ($rel = 4.12\times10^{-1}$, $PSNR = 21.98$)

scheme. Armijo's step lengths are $\alpha_1 = \alpha_2 = \ldots = \alpha_{10} = 1$, $\alpha_{11} = \frac{1}{2}$, $\alpha_{12} = \frac{1}{2^2}$, $\alpha_{13} = \ldots = \alpha_{16} = \frac{1}{2^3}$, $\alpha_{17} = \ldots = \alpha_{20} = \frac{1}{2^4}$, $\alpha_{21} = \alpha_{22} = \ldots = \alpha_{25} = \frac{1}{2^5}$, $\ldots$ and $|\,\|Af_{approx} - y\| - \delta| = 3513.3$. The relative accuracy for antireflective and reflective BCs for each case of Gaussian and *out-of-focus* blur are presented in Table 1. The relative error and *PSNR* of reconstructed image by applying the AR-BCs are 7.10×10^{-2} and 37.26 respectively as shown in Figure 1(b), while the reflective BC brings the result that the relative error is 4.12×10^{-1} and *PSNR* is 21.98 as shown in the reconstructed image of Figure 1(c). In this case, Armijo's step lengths are $\alpha_1 = \alpha_2 = \ldots = \alpha_{12} = 1$, $\alpha_{13} = \ldots = \alpha_{14} = \frac{1}{2}$, $\alpha_{15} = \ldots = \alpha_{17} = \frac{1}{2^2}$, $\alpha_{18} = \ldots = \alpha_{20} = \frac{1}{2^3}$, $\alpha_{21} = \alpha_{22} = \ldots = \alpha_{25} = \frac{1}{2^4}$, $\ldots$ and $|\,\|Ax_{approx} - y\| - \delta| = 17231.6$.

TABLE 1. Relative accuracy for antireflective and reflective BCs for each case of *Gaussian* and *out-of-focus* blur

Blur	Image	Antireflective BCs	Reflective BCs
Gaussian	planet	7.10×10^{-2}	4.12×10^{-1}
	text	6.87×10^{-1}	7.36×10^{-1}
	a	8.78×10^{-2}	6.51×10^{-1}
out-of-focus	planet	4.06×10^{-2}	4.49×10^{-1}
	text	7.32×10^{-1}	7.89×10^{-1}
	a	4.25×10^{-2}	1.95×10^{0}

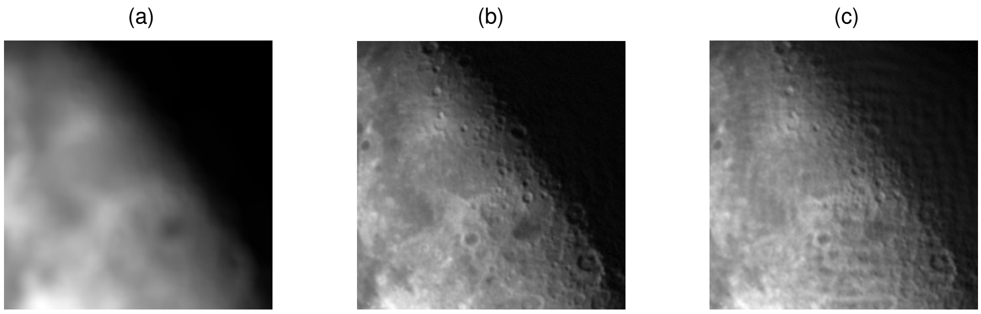

FIGURE 2. *Out-of-focus* blur : Restored image with (b) AR-BCs ($rel = 4.05 \times 10^{-2}$, $PSNR = 42.12$) and (c) reflective BCs ($rel = 4.48 \times 10^{-1}$, $PSNR = 21.24$)

The simulation results for *out-of-focus* blurring of the *planet* image are presented in Figure 2 and Table 1. By imposing the AR-BCs, the relative accuracy and the ringing effect are reduced. Consequently, the blurred *Planet* image is reconstructed by using the AR-BCs which is better than the reflective BCs.

As shown in Table 1 presenting the comparison of relative accuracy for three test images, the relative accuracy is smaller and *PSNR* is higher under the AR-BCs, and the more quality image under the AR-BCs for all three test images are obtained in our experiments. And there are little ringing effects in the reconstructed images from the AR-BCs . Thus AR-BCs brings the better results than reflective BCs in our experiments with three test images.

5. Conclusion

In the modelization of image deblurring, the choice of the most appropriate boundary conditions must be the one of the main aspect. Using the AR-BCs can eliminate the artificial boundary discontinuities. A large-scale ill-conditioned coefficient brought from the AR-BCs is related to the Toeplitz+Hankel plus 2 rank correction matrix. The fast truncated Lagrange(FTL) method is suitable to find appropriate solution of this system. Numerical results presented show that the AR-BCs provide an effective model for image restoration problems, for both the computational cost and minimizing the ringing effects near the boundary. Comparing reflective BCs, the AR-BCs provides the smaller relative accuracy and the higher *PSNR*.

The application of FTL algorithm to image restoring problem with the synthetic BCs can be our next research in the future.

References

[1] A. Arico, M. Donatelli, J. Nagy, and S. Serra-Capizzano, *The anti-reflective transform and regularization by filtering, Numerical Linear Algebra in Signals, Systems, and control*, Lecture Notes in Electrical Engineering **80**, Springer Verlag, (2011), 1-21.

[2] A. Arico, M. Donatelli, and S. Serra-Capizzano, *Spectral analysis of the antireflective algebra*, Linear Alg. and its Appl. **428** (2008), 657-675.
SIAM Review **52** (2010), no. 1, 113-147.

[3] M. Christiansen and M. Hanke, *Deblurring methods using anti-reflective boundary conditions,* SIAM J. Matrix Anal. Appl. **22** (2001), 1204-1221.

[4] M. Donatelli and S. Serra-Capizzano, *Anti-reflective boundary conditions and re-blurring,* Inverse Problem **21** (2005), 169-182.

[5] M. Donatelli, C. Estatico, and S. Serra-Capizzano, *Boundary conditions and multiple-image re-blurring: The LBT case,* J. of Comp. and Appl. Math. **198** (2006), 426-442.

[6] M. Donatelli, C. Estatico, A Martinelli, and S. Serra-Capizzano, *Improved image deblurring with anti-reflective boundary conditions and re-blurring,* Inverse Problem **22** (2006), 2035-2053.

[7] M. Donatelli and N. Mastronardi, *Fast deconvolution with approximated PSF by RSTLS with antireflective boundary conditions,* J. of Comp. and Appl. Math. **236** (2012), 3992-4005.

[8] M. Donatelli, http://scienze-como.uninsubria.it/mdonatelli/Software/software.html.

[9] R. C. Gonzalez and R. E. Woods, *Digital image processing,* Prentice Hall, 2002.

[10] P. C. Hansen, *Regularization Tools,* (2001), http://www.imm.dtu.dk/ pch.

[11] P. C. Hansen, *Deconvolution and Regularization with Toeplitz matrices,* Numerical Algorithms, **29** (2002), 323-378.

[12] P. C. Hansen, J. G. Nagy, and D. P. O'Leary, *Deblurring Images Matrices, Spectra, and Filtering*, SIAM, 2006.

[13] G. Landi, *A fast truncated Lagrange method for large-scale image restoration problems,* Applied Mathematics and Computation **186** (2007), 1075-1082.

[14] K. P. Lee, J. G. Nagy, and L. Perrone, *Iterative Methods for Image Restoration: A Matlab Object Oriented Approach,* Numerical Algorithms **36** (2004), 73-93.

[15] M. K. Ng, R. H. Chan, and W. C. Tang, *A fast algorithm for deblurring models with Neumann boundary conditions*, SIAM J. Sci. Comp. **21** (1999), no. 3, 851-866.

[16] M. K. Ng, W. C. Kwan, *Image restoration by cosine transform-based iterative regularization*, Applied Mathematics and Computation **160** (2005), 499-515.

[17] S. Y. Oh and S. J. Kwon, A fast Lagrange method for large-scale image restoration problems with reflective boundary condition, J. of Chungcheong Math. Soc. **25** (2012), 367-377.

[18] S. Serra-Cappizzano, *A note on antireflectibe boundary conditions and fast deblurring models*, SIAM J. Sci. Comp. **25** (1999), no. 4, 851-866.

[19] S. Serra-Capizzano, *A note on anti-reflective boundary conditions and fast deblurring models,* SIAM J. Sci. Comp. **25** (2003), no. 3, 1307-1325.

*

Department of Mathematics
Chungnam National University
Daejeon 34134, Republic of Korea
E-mail: soh@cnu.ac.kr

**

Innovation Center of Engineering Education
Chungnam National University
Daejeon 34134, Republic of Korea
E-mail: sjkw@cnu.ac.kr